Effects of Phosphorylation of Threonine 160 on Cyclin-dependent Kinase 2 Structure and Activity

Nicholas Brown, Martin E.M. Noble, Alison Lawrie, May Morris, Paul Tunnah, Gilles Divita, Louise Johnson, Jane Endicott

THE JOURNAL OF BIOLOGICAL CHEMISTRY
Vol. 274, No. 13, Issue of March 26, pp. 8746–8756, 1999

Printed in U.S.A.

Effects of Phosphorylation of Threonine 160 on Cyclin-dependent Kinase 2 Structure and Activity*

(Received for publication, September 30, 1998, and in revised form, November 18, 1998)

Nicholas R. Brown‡, Martin E. M. Noble‡, Alison M. Lawrie‡, May C. Morris§, Paul Tunnah‡, Gilles Divita§, Louise N. Johnson‡, and Jane A. Endicott‡¶

From the ‡Laboratory of Molecular Biophysics, Department of Biochemistry, and Oxford Centre for Molecular Sciences, University of Oxford, The Rex Richards Building, South Parks Road, Oxford OX1 3QU, United Kingdom and §Centre de Recherche de Biochemie Macromoleculaire, CNRS, Montpellier, 1919 Route de Mende, 34293 Montpellier Cedex, France

We have prepared phosphorylated cyclin-dependent protein kinase 2 (CDK2) for crystallization using the CDK-activating kinase 1 (CAK1) from *Saccharomyces cerevisiae* and have grown crystals using microseeding techniques. Phosphorylation of monomeric human CDK2 by CAK1 is more efficient than phosphorylation of the binary CDK2-cyclin A complex. Phosphorylated CDK2 exhibits histone H1 kinase activity corresponding to approximately 0.3% of that observed with the fully activated phosphorylated CDK2-cyclin A complex. Fluorescence measurements have shown that Thr^{160} phosphorylation increases the affinity of CDK2 for both histone substrate and ATP and decreases its affinity for ADP. By contrast, phosphorylation of CDK2 has a negligible effect on the affinity for cyclin A. The crystal structures of the ATP-bound forms of phosphorylated CDK2 and unphosphorylated CDK2 have been solved at 2.1-Å resolution. The structures are similar, with the major difference occurring in the activation segment, which is disordered in phosphorylated CDK2. The greater mobility of the activation segment in phosphorylated CDK2 and the absence of spontaneous crystallization suggest that phosphorylated CDK2 may adopt several different mobile states. The majority of these states are likely to correspond to inactive conformations, but a small fraction of phosphorylated CDK2 may be in an active conformation and hence explain the basal activity observed.

Progression through the eukaryotic cell cycle is critically dependent upon the activity of a family of serine/threonine kinases, the cyclin-dependent protein kinases (CDKs).[1] CDKs are regulated by both transcriptional and post-translational mechanisms that promote the correct timing and order of events for cell growth and cell division (1). Monomeric, nonphosphorylated CDKs have no detectable kinase activity. Activation requires two components: (i) the association of a positive regulatory cyclin subunit (2, 3) and (ii) activating phosphorylation of the kinase on a threonine residue (Thr^{160} in CDK2) located in a surface loop termed the activation segment (4–8).

In metazoans, a CDK-cyclin pair, CDK7-cyclin H, that requires a third protein, MAT-1, exhibits CDK-activating kinase (CAK) activity (9–16). CDK7 and cyclin H are also components of the multimeric basal transcription factor complex, TFIIH (17, 18). In *Saccharomyces cerevisiae*, CAK activity is associated with a monomeric protein called CAK1 or CIV1 (CAK *in vivo*) (19–21). CAK1 shows greatest sequence similarity to the CDK family but does not have a cyclin partner. Dephosphorylation of the threonine in the activation segment is catalyzed by the kinase-associated phosphatase (KAP) (22, 23). For CDK2, KAP will only accept monomeric phosphorylated CDK2 as a substrate and not the binary complex of phosphorylated CDK2-cyclin A, suggesting that *in vivo* KAP dephosphorylates Thr^{160} only after the cyclin subunit is dissociated or degraded. Cyclin proteolysis is mediated by the ubiquitin-dependent pathway (24–27). CDK-cyclin heterodimers may also be regulated by reversible phosphorylation at other sites leading to inhibition (reviewed in Ref. 1) and by association with protein inhibitor molecules (CKIs) such as p27^{kip1} (reviewed in Ref. 28).

Several groups have addressed the question of whether the monomeric CDK or the CDK-cyclin complex is the better substrate for phosphorylation by CAK. The results suggest both a CDK and species dependence. Studies using CAK purified from starfish oocytes (9) concluded that this enzyme can only phosphorylate CDC2 (CDK1) when it is bound to a cyclin. However, CAK purified from *Xenopus laevis* egg extract can phosphorylate bacterially expressed human CDK2 (10) or GST-CDK2 (11) in the absence of cyclin. Fisher and Morgan working with CAK purified from both human and murine cells have shown that CAK activates complexes of CDK2 and CDC2 with various cyclins and also phosphorylates CDK2, but not CDC2, in the absence of cyclin (12). Studies with *S. cerevisiae* CAK1 have indicated that CDK2 and CDC28 phosphorylation can occur with or without cyclin (19–21).

The requirement for CDKs to be both phosphorylated and associated with a cyclin subunit for full activation indicates that more significant changes need to occur than those promoted by phosphorylation alone. Other kinases such as cAMP-dependent protein kinase (29, 30), lymphocyte kinase, Lck (31), insulin receptor tyrosine kinase (32), and mitogen-activated protein kinase (33) are activated solely by phosphorylation without the need for association with another protein subunit. Kinase activity associated with monomeric phosphorylated CDKs has been reported for CDK7, where dual phosphorylation on the two sites in the activation segment (Ser^{170} and Thr^{176} in *X. laevis* CDK7) is sufficient to generate CAK activity to one-third of its maximal value *in vitro* (34). Monomeric

* This work was supported by the Medical Research Council, BBSRC, Royal Society, The Wellcome Trust, CNRS, ARC (contract 1244), and the Ligue Nationale Contre le Cancer. The costs of publication of this article were defrayed in part by the payment of page charges. This article must therefore be hereby marked "*advertisement*" in accordance with 18 U.S.C. Section 1734 solely to indicate this fact.

The atomic coordinates for the phosphorylated CDK2-ATP complex structure (1b39), its associated structure factors (r1b39sf), the nonphosphorylated CDK2-ATP complex (1b38), and its associated structure factors (r1b38sf) have been deposited in the Protein Data Bank, Brookhaven National Laboratory, Upton, NY.

¶ To whom correspondence should be addressed.

[1] The abbreviations used are: CDK, cyclin-dependent kinase; CAK, CDK-activating kinase; GST, glutathione S-transferase; PAGE, polyacrylamide gel electrophoresis; KAP, kinase-associated phosphatase; Mant, 2′(3′)-*O*-(*N*-methylanthraniloyl).

TABLE I
Statistics of the data sets used and of the refined structures

Parameter	Data collected (Space group $P2_12_12_1$)	
	CDK2-ATP	Phosphorylated CDK2-ATP
Cell dimensions (Å)	53.33, 71.12, 72.19	53.42, 71.66, 72.52
Maximal resolution (Å)	2.00	2.10
Observations	70,729	70,130
Unique reflections, completeness (%)	18,076 (95.2%)	15,947 (96.3%)
R_{merge} [a]	0.092	0.124
Mean $I/\sigma(I)$	11.01	4.1
Highest resolution bin (Å)	2.10–2.00	2.23–2.11
Completeness (%)	96.8%	97.2%
Mean I/mean $\sigma(I)$	2.26	2.0
R_{merge}	0.390	0.375
Refinement statistics		
Protein atoms	2338	2338
Residues	1–35, 44–298	1–35, 44–298
Other atoms	206 water	145 water
	31 ATP	31 ATP
	1 Mg	1 Mg
Resolution range (Å)	20.00–2.10	20.00–2.10
R_{conv} [b]	0.18	0.20
R_{free} [c]	0.25	0.27
Mean protein temperature factors $(Å)^2$	27.3	31.0
Mean ligand temperature factors $(Å)^2$	28.3	44.5

[a] $R_{merge} = \Sigma_h \Sigma_j |I_{h,j} - \bar{I}_h| / \Sigma_h \Sigma_j I_{h,j}$, where $I_{h,j}$ is the intensity of the jth observation of unique reflection h.
[b] $R_{conv} = \Sigma_h ||F_{Oh}| - |F_{Ch}|| / \Sigma_h |F_{Oh}|$, where F_{Oh} and F_{Ch} are the observed and calculated structure factor amplitudes for reflection h.
[c] R_{free} is equivalent to R_{conv} but is calculated using a 5% disjoint set of reflections excluded from the least squares refinement stages.

phosphorylated CDK2 has been reported to be inactive (12).

Crystallographic studies on CDK2 have provided a detailed understanding of the basis of CDK2 activation by cyclin A binding and phosphorylation (35–37). CDK2 adopts a characteristic protein kinase fold composed of a mostly β-sheet N-terminal domain that contains one helix, the C-helix, and a predominantly α-helical C-terminal domain. The ATP-binding site is situated at the domain-domain interface. In the structure of inactive, monomeric CDK2, residues at the ATP-binding site are wrongly disposed and are unable to promote the correct alignment of the triphosphate moiety for catalysis, although the inactive monomer can bind ATP (35). The inactive conformation arises mainly from the organization of two key elements of structure. These are the C-helix, which contains the PSTAIRE motif (single letter amino acid code, residues 45–51), and the activation segment, which includes residues that lie between the conserved DFG and APE motifs (residues 145–147 and 170–172, respectively). The position of the C-helix in the inactive CDK2 monomer results in the loss of the stabilizing interaction between Glu^{51} (the E of the PSTAIRE sequence) and Lys^{33} that is important for correct localization of the ATP triphosphate. The activation segment conformation buries Thr^{160} away from solvent facing in toward the conserved glycine-rich loop.

Upon formation of the CDK2-cyclin A complex, there are no changes in the structure of cyclin A (38), but there are substantial changes in CDK2 that create the ATP triphosphate recognition site (36). CDK2-cyclin A exhibits about 0.2% of the activity of the fully activated phosphorylated binary complex. In the structure of phosphorylated CDK2-cyclin A, further structural rearrangements occur centered within the activation segment (37). Thr^{160}, now phosphorylated, turns in to contact three arginine residues: one (Arg^{50}) from the C-helix PSTAIRE motif within the N-terminal domain, a second (Arg^{126}) that is adjacent to the catalytic aspartate (Asp^{127}), and a third (Arg^{150}) from the start of the activation segment. The phosphothreonine group acts as an organizing center, and a major outcome of the realigned phosphorylated CDK2-cyclin A structure appears to be the formation of the protein-substrate recognition site that is likely to depend most sensitively on the activation segment orientation.

In order to elucidate the structure and biological properties of phosphorylated CDK2 in the absence of cyclin, we have prepared phosphorylated CDK2 by the action of CAK1 on CDK2. We have analyzed the role of cyclin in the recognition of CDK2 by CAK1; the relative affinities of CDK2 and phosphorylated CDK2 for cyclin A, ATP, and substrate; and the structural consequences of CDK2 phosphorylation. The crystallographic results demonstrate disorder in the activation segment of phosphorylated CDK2 compared with this region of nonphosphorylated CDK2. We propose that this disorder can explain the differences observed in ATP and substrate binding between phosphorylated and nonphosphorylated CDK2 and the low level of phosphorylated CDK2 histone H1 kinase activity.

EXPERIMENTAL PROCEDURES

Protein Expression and Purification

Human CDK2 was expressed in Sf9 insect cells using a recombinant baculovirus encoding CDK2 (*Autographica californica* CDK2) following slight modifications to the published method (39). Briefly, Sf9 cells, adapted to Sf900-II serum-free medium (Life Technologies, Inc.), were maintained in shake flasks at 28 °C. Cells (2×10^9) were infected with *A. californica* CDK2 at a multiplicity of infection of 10. At 48 h postinfection, the virus-infected cells were harvested and lysed in hypotonic lysis buffer (25 mM NaCl, 1 mM EDTA, 1 μg/ml pepstatin, 1 μg/ml leupeptin, 0.1 mM benzamidine, 10 mM Tris-HCl, pH 7.4). After homogenization, the lysate was clarified by centrifugation (100,000 × *g* for 1 h at 4 °C) and loaded onto DEAE-Sepharose (1.6 × 13 cm; Amersham Pharmacia Biotech), preequilibrated in hypotonic lysis buffer. The NaCl concentration of the flow-through pool was raised to 50 mM prior to loading onto an SP-Sepharose column (1.6 × 30 cm, Amersham Pharmacia Biotech). CDK2 eluted in the flow-through as two distinct peaks that were pooled separately and then further purified using an ATP-agarose column (11-atom spacer, ribose hydroxyl-linked, 1 × 5 cm; Sigma) preequilibrated in 25 mM NaCl, 1 mM EDTA, 1 mM dithiothreitol, 10% glycerol, 10 mM HEPES, pH 7.4. CDK2 was eluted with an increasing NaCl gradient. The two CDK2 populations eluting from the SP-Sepharose column behaved equivalently on the ATP-agarose column, and both pools were successfully phosphorylated by CAK1.

Human CDK2 was also prepared as a GST fusion protein using a pGEX-KG plasmid transformed into *Escherichia coli* strain JM101. 1-Liter cultures were induced with 0.1 mM isopropyl-1-thio-β-D-galactopyranoside and incubated for 16 h at 25 °C. Harvested cells were lysed by sonication of a freeze/thawed sample to which lysozyme (0.1 mg/ml) had been added. Following clarification, the lysate was applied to a 5-ml glutathione-Sepharose column (Amersham Pharmacia Bio-

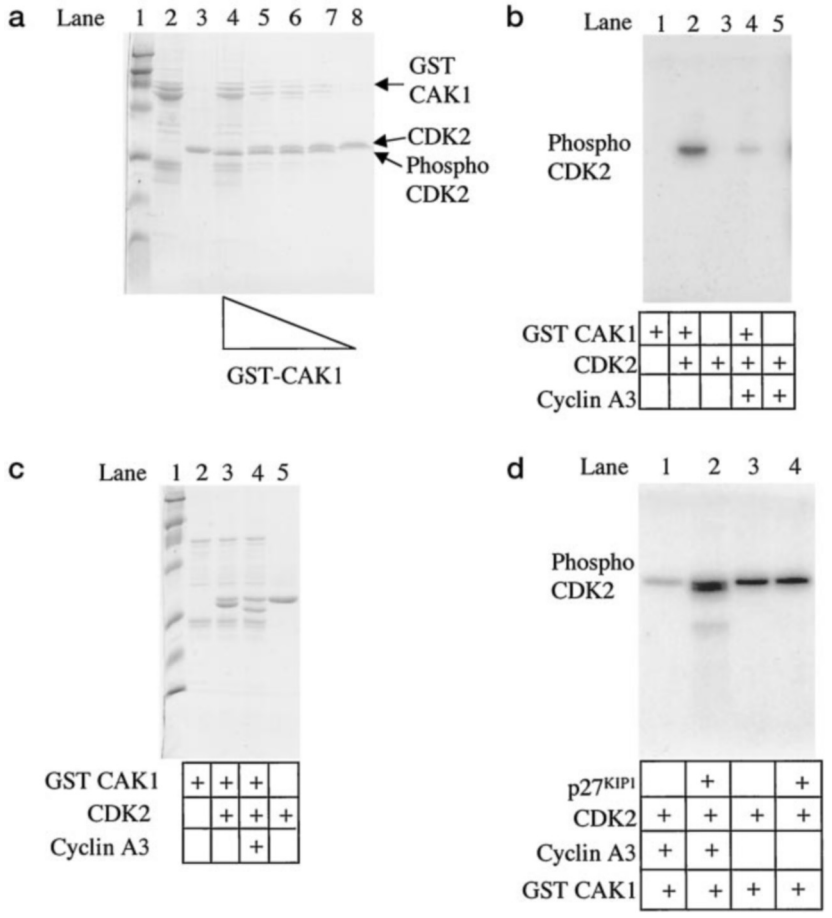

FIG. 1. *a*, phosphorylation of CDK2 by GST-CAK1. *Lane 1*, molecular weight markers. Markers are at 200, 98, 66, 45, 30, 20, and 12 kDa. *Lane 2*, GST-CAK1. *Lane 3*, monomeric CDK2. Different concentrations of GST-CAK1 (7.5, 3.0, 1.5, 0.75, and 0.12 μM GST-CAK1 in *lanes 4–8*, respectively) were co-incubated with 30 μM monomeric CDK2. Proteins were visualized by Coomassie stain following 15% SDS-PAGE. As shown, phosphorylated CDK2 has a higher electrophoretic mobility by SDS-PAGE than unphosphorylated CDK2. *b*,CAK1-catalyzed incorporation of ^{32}P from γ-labeled ATP into monomeric CDK2. CDK2 was phosphorylated by coincubation with GST-CAK1 in the absence (*lane 2*) or presence (*lane 4*) of cyclin A3. The GST-CAK1 (*lane 1*), CDK2 (*lane 3*), or CDK2-cyclin A3 (*lane 5*) samples show no autophosphorylation activity. *c*, comparative study of CDK2 and CDK2-cyclin A3 phosphorylation by CAK1. Monomeric CDK2 is a more efficient substrate for CAK1-catalyzed phosphorylation than the binary CDK2-cyclin A3 complex. *Lane 1*, molecular weight markers; *lane 2*, GST-CAK1; *lane 3*, CDK2 co-incubated with CAK1; *lane 4*, CDK2-cyclin A3 complex with CAK1; *lane 5*, CDK2. All reactions were carried out under the conditions described under "Experimental Procedures." *d*, effect of p27^{kip1} upon phosphorylation of CDK2 by GST-CAK1 in the presence and absence of cyclin A3. CDK2 (0.3 μM) was incubated with GST-CAK1 (0.1 μM) in the presence and absence of p27^{kip1} (50 nM) and cyclin A3 (0.3 μM), and the reaction was allowed to proceed as described under "Experimental Procedures." Enhancement of phosphorylation of the CDK2-cyclin A3 binary complex to levels observed for the monomeric CDK2 is seen in the presence of p27^{kip1} (compare *lanes 1* and *2*). In this experiment, p27^{kip1} was also labeled and is apparent just *below* the phosphorylated CDK2 band in *lane 2*. No difference is seen when using monomeric CDK2 as a substrate (compare *lanes 3* and *4*).

tech) preequilibrated in Hepes-buffered saline (10 mM Hepes, pH 7.4, 134 mM NaCl, 2 mM EDTA), and after washing, the GST fusion protein eluted with freshly prepared Hepes-buffered saline containing 20 mM glutathione. Yields of soluble fusion were greater than 100 mg/liter. Following thrombin cleavage (Sigma; 16 h at 1:1000 (w/w) at 25 °C), CDK2 was purified by gel filtration (Superdex 75; Amersham Pharmacia Biotech) and glutathione-Sepharose (Amersham Pharmacia Biotech).

A C-terminal fragment (residues 171–432) of bovine cyclin A, cyclin A3, possessing a hexahistidine tag, was expressed and purified as described (38).

A pGEX clone containing the CAK1 cDNA insert was transformed into *E. coli* strain B834. Typically 1–2 liters of bacterial culture were grown to an A_{600} of 0.7 at 37 °C and then shifted to 16 °C for 2 h before induction with 0.4 mM isopropyl-1-thio-β-D-galactopyranoside and incubation for a further 28 h at 16 °C. Harvested cells were lysed, and GST-CAK1 was purified using glutathione-Sepharose as described above. Yields of soluble fusion protein were 2 mg/liter. The partially purified preparation showed three bands around the expected position of the fusion protein on gels. Thrombin digests demonstrated that the middle band was GST-CAK1. Since the preparation was an effective source of CAK activity, further purification was not carried out. Partially purified fusion was found to be stable for at least 2 weeks when stored on ice.

His-tagged CAK1 was overexpressed in *S. cerevisiae* strain MD4/4C

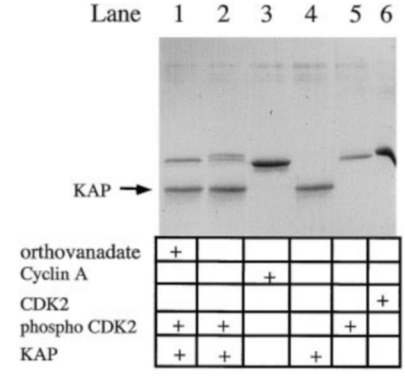

FIG. 2. **CDK-associated phosphatase KAP dephosphorylates phosphorylated CDK2.** KAP specifically dephosphorylates monomeric phosphorylated CDK2. CDK2, phosphorylated CDK2, cyclin A3, KAP, and orthovanadate were co-incubated as indicated and under conditions as described under "Experimental Procedures."

(α leu2 his3 ura2 trp1) as described (20). The cell lysate was loaded onto a nickel-nitrilotriacetic acid resin (Qiagen) and purified according to the manufacturer's instructions. The His-tagged CAK1 showed similar en-

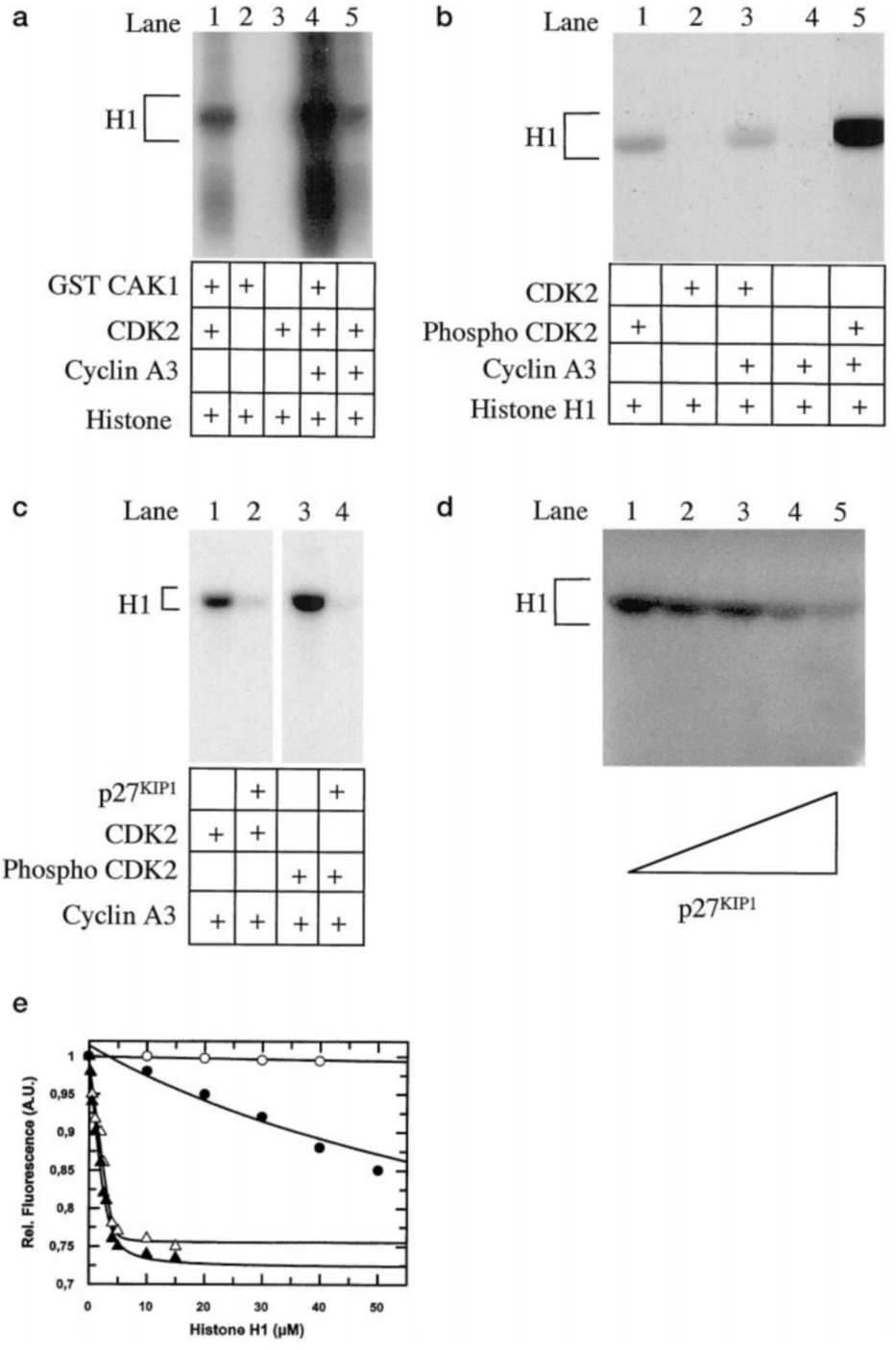

FIG. 3. *a*, CDK2 phosphorylated on Thr^{160} has partial histone H1 kinase activity. CDK2, cyclin A3, GST-CAK1, and histone H1 were co-incubated in various combinations as indicated in the presence of radiolabeled [^{32}P]ATP and under conditions as described under "Experimental Procedures." Radiolabeled histone H1 was visualized following 15% SDS-PAGE and autoradiography. *b*, CDK2 expressed in *E. coli* cells is a substrate for CAK1. The experiment described in *a* above was repeated using CDK2 synthesized in *E. coli* cells. *c*, the histone kinase activity of phosphorylated CDK2-cyclin A3 and CDK2-cyclin A3 are inhibited by p27^{kip1}. p27^{kip1} (0.5 μM) inhibits both phosphorylated and nonphosphorylated binary complexes (0.3 μM) (compare *lanes 1* and *2* and *lanes 3* and *4*, respectively). *d*, the histone kinase activity of phosphorylated CDK2 is inhibited by p27^{kip1}. The addition of increasing quantities of p27^{kip1} (5 nM, 50 nM, 500 nM, and 5 μM) to 50 nM phosphorylated monomeric CDK2 (*lanes 2–5*) revealed that 5 μM p27^{kip1} showed strong inhibitory activity. *e*, binding of histone H1 to CDK2. A fixed (0.1 μM) concentration of CDK2 (○), phosphorylated CDK2 (●), CDK2-cyclin A (△), and phosphorylated CDK2-cyclin A (▲) were titrated by increasing concentration of histone H1. The binding was monitored by following the quenching of intrinsic fluorescence at 340 nM, and the data were fitted according to a quadratic equation that assumes the presence of a single site for histone H1.

zymatic properties to those of the fusion protein.

CDK2 phosphorylated on Thr^{160} was prepared by adding CAK1 activity (either as GST fusion or a histidine-tagged version) at a final CAK1:CDK2 ratio of between 1:20 and 1:2 (w/w) in the presence of 50 mM Tris-HCl, pH 7.5, 10 mM magnesium chloride, 1 mM ATP for 0.5 h at 25 °C. As reported by others (19, 20), we also found that CAK1 gave a burst of phosphorylation followed by a fall in activity within minutes (data not shown). In order to obtain complete phosphorylation of CDK2, 3–4 aliquots of CAK1 and ATP were added. With GST-CAK1, ratios of 1:2 were required to achieve complete phosphorylation as judged by band shift on SDS-PAGE. Phosphorylated CDK2 was purified for analysis and crystallization trials by gel filtration (Superdex 75; Amersham Pharmacia Biotech), a step that removed high molecular weight contaminants and glutathione. A glutathione-Sepharose column (Amersham Pharmacia Biotech) was then used to remove GST-CAK1. With histidine-tagged CAK1, lower amounts of CAK1 to CDK2 were used (1:20), and ion exchange (MonoQ; Amersham Pharmacia Biotech) was employed to resolve phosphorylated CDK2 from unmodified CDK2 and His-tagged CAK1. The reaction mixture was dialyzed against 25 mM Tris-HCl, pH 8.5, containing 1 mM EDTA and 1 mM monothiolglycerol before loading onto the ion exchanger equilibrated in the same buffer. Pure phosphorylated CDK2, as judged by SDS-PAGE, eluted at approximately 75 mM salt upon gradient elution.

Binary complexes of CDK2-cyclin A3 and phosphorylated CDK2-cyclin A3 were formed by adding cyclin A3 in slight molar excess to the CDK2 subunit and purified by Superdex 75 gel filtration chromatography. Human p27^{kip1} carrying a C-terminal His$_6$ tag was expressed in *E. coli* cells (0.1 mM isopropyl-1-thio-β-D-galactopyranoside, 3–4 h at 37 °C) and purified in one step using nickel-nitrilotriacetic acid resin. Purified recombinant KAP was a kind gift of Dr. Neil Hanlon.

Kinase Assays

Phosphorylation of CDK2 was monitored by gel shift on SDS-PAGE using 15% acrylamide and also by incorporation of ^{32}P-labeled phosphate. Initially GST-CAK1 was titrated, at concentrations from 0.75 to

7.5 μM (50–500 ng in 10 μl), against 30 μM (1 μg in 10 μl) monomeric CDK2 as substrate. Kinase reactions were performed in 10 μl of buffer containing 50 mM Tris-HCl, pH 7.5, 10 mM magnesium chloride, 1.0 mM ATP for 30 min at 30 °C.

Radioactive analytical kinase reactions were performed using 1.5 μM GST-CAK1 (100 ng in 10 μl) in 50 mM Tris-HCl, pH 7.5, 10 mM magnesium chloride, 0.1 mM ATP containing 1 μCi of γ-^{32}P-labeled ATP (Amersham Pharmacia Biotech) and either 15 μM CDK2-cyclin A3 complex (1 μg in 10 μl) or 15 μM monomeric CDK2 (0.5 μg in 10 μl) as substrate. The reactions proceeded for 30 min at 30 °C before termination with SDS sample buffer. Following SDS-PAGE (15% acrylamide), the stained and dried gels were subjected to autoradiography. Histone H1 kinase activity was examined using the same reaction conditions to which 300 μM histone H1 (Boehringer Mannheim) was added. Inhibition of kinase activity by p27^{kip1} was measured by including 35 μM p27^{kip1} (1.0 μg in 10 μl) in the radioactive kinase assays carried out under the same reaction conditions as described above. PhosphorImager analyses (Molecular Dynamics, Inc., Sunnyvale, CA) were carried out on the fixed, stained, and dried gels.

Dephosphorylation of Phosphorylated CDK2 by KAP

15 μM purified phosphorylated CDK2 (0.5 μg in 10 μl) was incubated with 25 μM KAP (0.6 μg in 10 μl) in a buffer containing 50 mM Tris-HCl, pH 7.5, in the presence or absence of 1 mM sodium orthovanadate. The reaction was stopped after 1 h at 25 °C by the addition of SDS sample buffer. Samples were analyzed by SDS-PAGE (15% acrylamide).

Analysis of CDK/Nucleotide Interactions

2′(3′)-*O*-(*N*-methylanthraniloyl) (Mant)-derivated nucleotide analogues were synthesized as described by Hiratsuka (40) and purified according to John *et al*. (41). Cyclin A was overexpressed in *E. coli* and purified to homogeneity as described by Lorca *et al.* (42). Fluorescence measurements were performed at 25 °C using a Spex II fluorolog spectrofluorometer, with spectral band passes of 2 and 8 nm, for excitation and emission, respectively. The intrinsic tryptophan fluorescence of CDK2 (0.2 μM of protein) was measured in a fluorescence buffer containing 50 mM Tris-HCl, pH 7.5, 50 mM KCl, 5% glycerol, and 2 mM EDTA. Proteins were incubated for 30 min in fluorescence buffer before starting the experiments, and all measurements were corrected as already described (43). The binding of ATP and ADP was monitored by the quenching of the intrinsic tryptophan fluorescence of CDK2 at 340 nm upon excitation at 295 nm. A fixed concentration of CDK2 (0.2 μM) was titrated by increasing the concentration of ATP or ADP, respectively. The binding of Mant-nucleotides to CDK2 was monitored by the enhancement of the Mant-group fluorescence at 450 nm upon excitation at 340 nm (41). Titration curve fitting was accomplished using Grafit software (Erithacus Software Ltd.) using a quadratic equation (44). All the results correspond to the average of four separate experiments with an S.D. value lower than 10% for intrinsic and extrinsic fluorescence titrations.

Analysis of CDK/Cyclin Interactions

Fluorescence Experiments—The affinity between CDK2 or phosphorylated CDK2 and cyclin A was measured by the direct fluorescence titration of the CDK2-Mant-ATP complex with different cyclin A concentrations. Mant-ATP-CDK2 complexes were incubated for 15 min in the presence of different cyclin concentrations before starting the experiment. CDK2/cyclin interactions were also monitored using the enhancement of Mant-ATP fluorescence at 430 nm. The Mant-ATP-CDK2 complexes were kept at a constant concentration of 0.2 μM, and the fluorescence emission was monitored at 430 nm (excitation at 350 nm) as a function of the cyclin concentration. The K_d was calculated by fitting the data to a standard quadratic equation (44). For displacement experiments, CDK2-Mant-ATP complexes at a concentration of 0.2 μM were incubated in the presence of a 200-fold excess of ATP and with or without added cyclin A (200 nM). Dissociation of the fluorescently labeled nucleotides was monitored according to the quenching of Mant fluorescence at 430 nm upon excitation at 350 nm. Data were fitted as already described (44).

BIAcore Analysis—GST-CDK2 was used for BIAcore analysis because neither free cyclin A3 nor CDK2 could be immobilized in an active form. GST-CDK2 was phosphorylated by His-tagged CAK1, as described above, and the fusion protein was purified on Superdex 200 (Amersham Pharmacia Biotech). Phosphorylated GST-CDK2 showed minimal mobility shifts on SDS-PAGE. Phosphorylation of the CDK2 fusion protein was confirmed using γ-^{32}P-labeled ATP (Amersham Pharmacia Biotech). Samples of GST-CDK2 and GST-phosphorylated CDK2 were captured on the sensor chip (CM5) using immobilized anti-GST immunoglobulin (Amersham Pharmacia Biotech). Cyclin A3, at concentrations of 5–100 μg/ml, was passed over the chip at a flow rate of 5 μl/min. Data analysis was performed with the BIAevaluation software (version 2.1, Amersham Pharmacia Biotech).

TABLE II
Affinity constants of CDK2 and CDK2-cyclin A complexes for nucleotides and fluorescent analogues and histone H1

Values are given as calculated K_d (μM).

	CDK2	Phosphorylated CDK2	CDK2 + cyclin A	Phosphorylated CDK2 + cyclin A
			μM	
Substrate				
ATP	0.254	0.120	—[a]	—
ADP	1.4	6.7	—	—
Mant-ATP	0.256	0.170	—	—
Mant-ADP	1.5	5.4	—	—
Histone H1	ND[b]	100	1	0.7

[a] —, not determined.
[b] None detected.

Phosphorylated CDK2 Crystallization

Purified phosphorylated CDK2 was buffer-exchanged into 50 mM Tris-HCl, pH 7.5, 50 mM NaCl, 1 mM EDTA, 1 mM monothioglycerol and concentrated to 10 mg/ml using a Centricon 10 concentrator (Amicon). Since initial crystallization trials with phosphorylated CDK2 were not successful, sitting drops (2 μl) were prepared by mixing equal volumes of protein and well solution (12–16% PEG 4000, 0.1 M Tris-HCl, pH 7.5, 50 mM ammonium acetate) and allowed to equilibrate for 3 days before streak/microseeding with microcrystalline preparations of unmodified CDK2 using a 50-μm diameter steel wire for the seed transfer. Typically, crystals appeared within 2 days and continued to grow for 1 week. Maximum crystal dimensions were 200 × 100 × 75 μm. CDK2 was crystallized using the hanging drop method by mixing equal volumes (1 μl) of protein solution (at a concentration of 10 mg/ml in 15 mM NaCl, 10 mM HEPES, pH 7.4) and well solution (10–15% PEG 3350, 50 mM ammonium acetate, 0.1 M HEPES, pH 7.4). Crystals appeared overnight and continued to grow for 5 days. Crystal complexes of phosphorylated CDK2 and ATP and of CDK2 and ATP were prepared by soaking crystals in the presence of 2.5 mM ATP and 5 mM $MgCl_2$.

Data Collection and Processing

Data for the Phosphorylated CDK2-ATP complex were collected on beamline BW7B at DESY (Hamburg) operating at a wavelength of 1.044 Å using a 30-cm Mar Research image plate, oscillations of 1.0°, and exposure time of 120 s. The CDK2-ATP complex data set was collected on beamline 9.5 at the SRS operating at a wavelength of 1.20 Å using a 30-cm Mar Research image plate, oscillations of 1.0°, and an exposure time of 450 s/frame. In each case, data were collected at 100 K after crystals had been transferred briefly to cryoprotectant (mother liquor containing 20% glycerol) and then mounted using a nylon loop. Images were integrated with the DENZO package and subsequently scaled and merged using SCALEPACK (45). Statistics of the data sets used are given in Table I.

Structure Solution and Refinement

Identical protocols were used for the refinement of phosphorylated CDK2-ATP and unphosphorylated CDK2-ATP structures. The starting model for refinement was the structure of CDK2 in complex with a purine-based inhibitor refined at 1.3-Å resolution.[2] This model included protein residues 1–35 and 44–298. Residues 36–43, prior to the C-helix, are disordered and have not been built in any reported monomeric CDK2 structure. At first, rigid body refinement of this model against the two data sets was performed. As the resolution of the data included was increased from 3.0 to 2.1 Å, an increasing number of rigid bodies was used, so that initially the whole molecule was treated as a single rigid body, and finally five amino acid segments were allowed to refine independently. Refinement of the models was then pursued with alternating cycles of interactive model building (46) and maximum likelihood refinement using the program REFMAC (47). In all cases where manual intervention was required, the structural changes indicated were similar for both structures. No electron density trace could be seen

[2] M. E. M. Noble, A. M. Lawrie, P. Tunnah, L. N. Johnson, and J. A. Endicott, unpublished results.

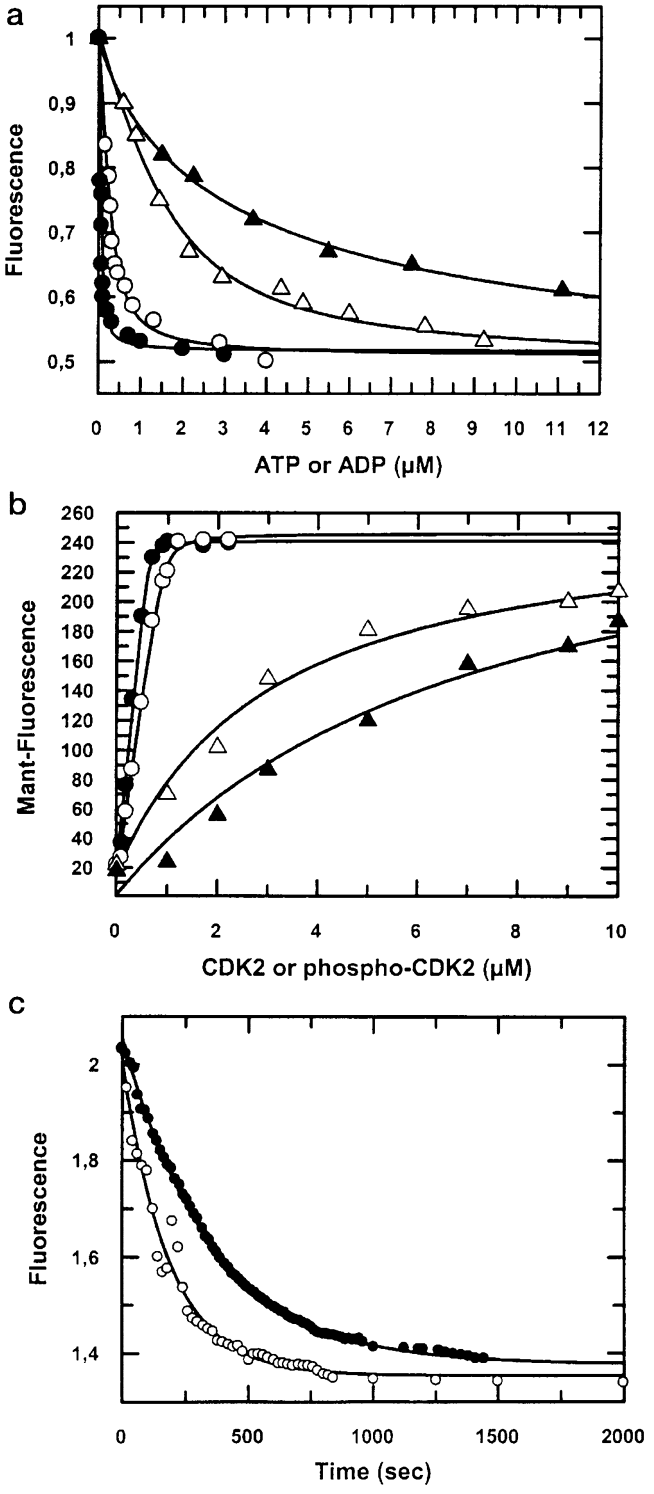

FIG. 4. *a*, nucleotide binding to CDK2 and phosphorylated CDK2. ATP or ADP binding to phosphorylated CDK2 was monitored by following the quenching of intrinsic tryptophan fluorescence at 340 nm upon excitation at 290 nm. A fixed concentration of CDK2 (0.2 μM) (*open symbols*) and phosphorylated CDK2 (*closed symbols*) were titrated with increasing concentrations of ATP (○, ●) and ADP (△, ▲). *b*, Mant-ATP and Mant-ADP binding to CDK2 and phosphorylated CDK2. Mant-nucleotides binding to either CDK2 or phosphorylated CDK2 result in an increase in the fluorescence of the Mant-group at 440 nm upon excitation at 350 nm. A fixed concentration of Mant-nucleotide (0.2 μM) (ATP (○, ●), ADP (△, ▲)) was titrated with increasing concentrations of CDK2 (*open symbols*), or phosphorylated CDK2 (*closed symbols*). *c*, Mant-ATP displacement from CDK2 and phosphorylated CDK2. Mant-ATP displacement from CDK2 (○) and phosphorylated CDK2 (●) by a 200-fold excess of ATP was monitored using the decrease of the Mant fluorescence at 450 nm. The dissociation kinetics were fitted as a single exponential to a rate constant of 5.2×10^{-3} s^{-1} and 3.1×10^{-3} s^{-1} for CDK2 and phosphorylated CDK2, respectively.

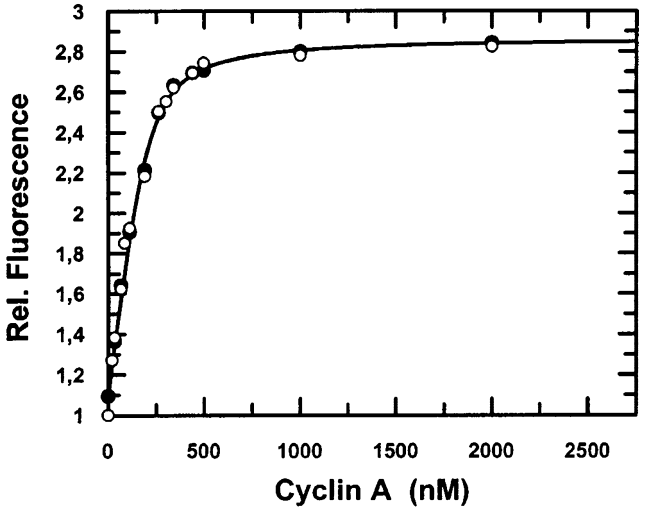

FIG. 5. **CDK2 and phosphorylated CDK2 binding to cyclin A3.** Binding titration of cyclin A to phosphorylated CDK2 was followed by Mant-ATP fluorescence enhancement. CDK2 (○) and phosphorylated CDK2 (●) previously saturated with Mant-ATP (1 μM) were titrated by increasing concentrations of cyclin A. The binding of cyclin A to CDK2 enhances the bound Mant-ATP fluorescence 3-fold at 440 nm upon excitation at 350 nm. The titration curves followed a monophasic pattern, with K_d values of 52 nM for CDK2-cyclin A and 48 nM for phosphorylated CDK2-cyclin A. In both cases, the stoichiometry of binding is 1:1 (CDK/cyclin). Cyclin binding is unaffected by Thr^{160} phosphorylation of CDK2.

for the tip of the activation segment (residues 153–164) of the phosphorylated CDK2-ATP structure, and neither omit refinement nor refinement of this region in alternative conformations could produce such a trace. The initial coordinates of MgATP were taken from the structure of CDK2-ATP determined by DeBondt *et al.* (35), and optimal geometry for this ligand was taken from the default PROTIN dictionary. Toward the end of the refinement, water molecules were added using ARP (48). Statistics of the final models are given in Table I.

RESULTS

Monomeric CDK2 is a Substrate for CAK1—Phosphorylation of CDK2 on Thr^{160} results in increased electrophoretic mobility of CDK2 on SDS-PAGE (Fig. 1*a*) (9, 12). We used this band shift to follow CDK2 phosphorylation by *S. cerevisiae* CAK1. The GST-CAK1 preparation contained several contaminants (see Fig. 1*a*, *lane 2*, and "Experimental Procedures") but provided a good source of CAK activity, and no further purification steps were introduced at this stage. CDK2 phosphorylation was also monitored by incorporation of ^{32}P from γ-labeled ATP (Fig. 1*b*). Radiolabeled phosphorylated CDK2 co-migrated with the faster migrating CDK2 band seen on Coomassie-stained gels. Comparative studies showed that monomeric human CDK2 is a better substrate for CAK1 than the human CDK2-bovine cyclin A3 complex as judged by both incorporation of ^{32}P (Fig. 1*b*) and mobility shift (Fig. 1*c*). Cyclin A3 migrates as a faster band than CDK2 or phosphorylated CDK2 (Fig. 1*c*, *lane 4*). (Bovine cyclin A3 corresponds to human cyclin A residues 171–432.) The addition of the CKI, $p27^{kip1}$ to monomeric CDK2 had no effect on the phosphorylation of Thr^{160} by GST-CAK1. However, $p27^{kip1}$ addition to the binary complex enhanced phosphorylation by CAK1 to levels observed with monomeric CDK2 (Fig. 1*d*). In these experiments, there was no evidence of radiolabeling of CAK1 by either phosphorylated CDK2 or phosphorylated CDK2-cyclin A3 (Fig. 1*b*). Similar results were obtained using His-tagged CAK1 expressed in *S. cerevisiae* as a source of

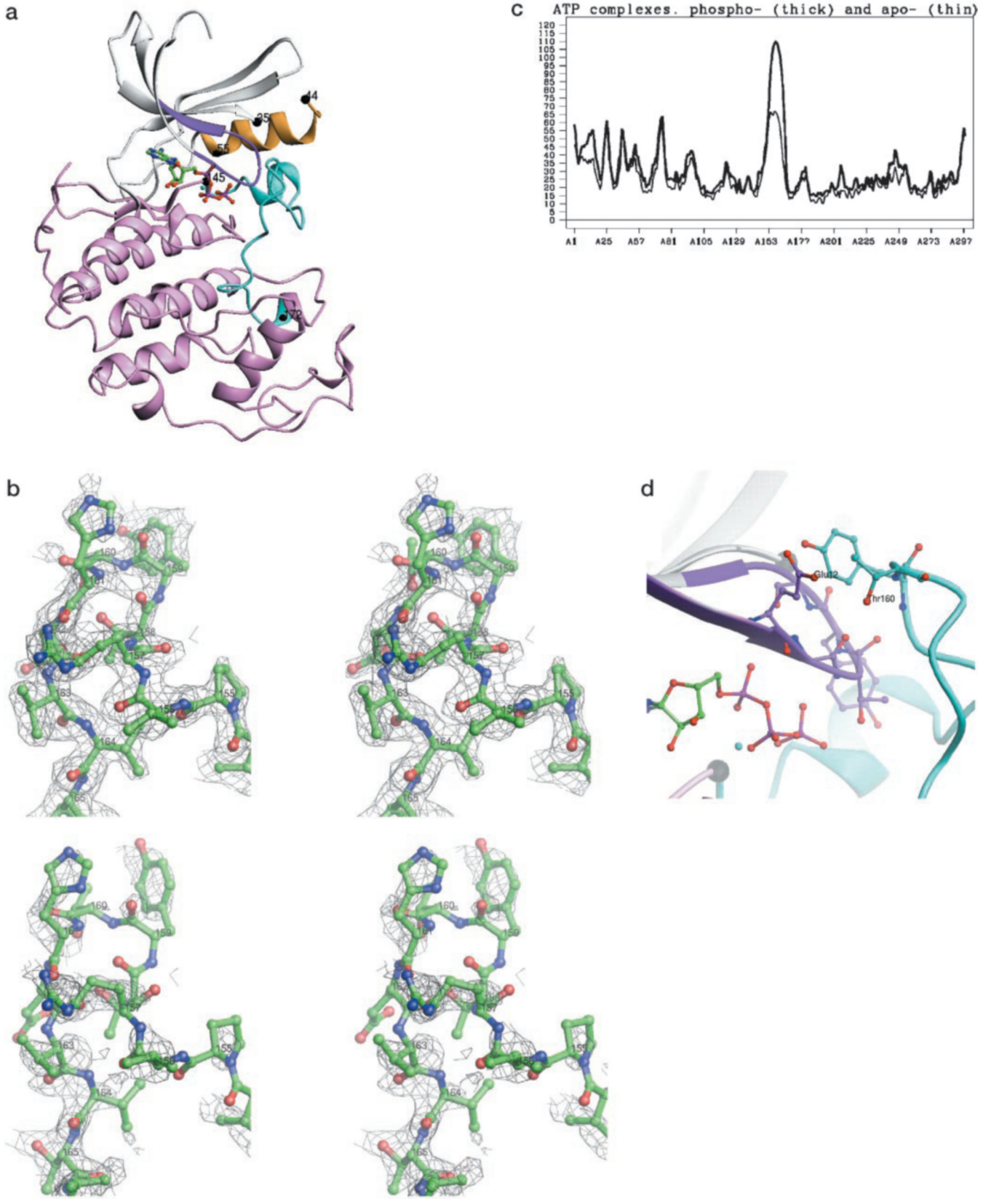

FIG. 6. *a*, the fold of monomeric CDK2. The structure is shown in a schematic representation with regions of β-sheet shown as *arrows* and α-helix shown as *ribbons*. The N-terminal domain is colored principally *white*, with the exception of the glycine-rich loop (colored *magenta*), and the C-helix (PSTAIRE helix, colored *gold*). The region of the N-terminal domain for which no trace is visible (residues 36–43) is indicated by *small black spheres* identifying residues 35 and 44. ATP is shown in *ball and stick* representation at the interface between the N- and C-terminal domains. The C-terminal domain is colored *pink*, with the activation segment (residues 145–172) highlighted in *cyan*. *b*, comparison of electron density for the tip of the activation segment. The *upper stereo pair* shows electron density defining the conformation of residues at the tip of the activation segment (residues 155–165) in the ATP complex of unphosphorylated monomeric CDK2, while the *lower stereo pair* shows the equivalent electron density in phosphorylated monomeric CDK2. In this *figure* the phosphate group attached to Thr^{160} has been omitted from the phosphorylated CDK2 structure for clarity. The maps were calculated using $(2F_o - F_c)\alpha_{calc}$ coefficients generated by REFMAC and are contoured at a level of $0.2e^{-}$ Å^{-3}.

CAK activity (results not shown). CDK2 phosphorylated by CAK1 was used to prepare phosphorylated CDK2 crystals.

As an additional test for CAK1 specificity, purified phosphorylated CDK2 was treated with the CDK-associated phosphatase, KAP. This enzyme specifically dephosphorylates monomeric phosphorylated CDK2 at Thr^{160} but shows no activity toward phosphorylated CDK2-cyclin A (24). Incubation of monomeric phosphorylated CDK2 with purified recombinant KAP resulted in a gel shift to a position characteristic of unmodified CDK2 (Fig. 2).

Mass spectroscopic analysis of phosphorylated CDK2 was used as a final test for CAK1 specificity. The results of this analysis (not shown) confirmed that CDK2 incubated with CAK1 is only phosphorylated on residue Thr^{160}.

CDK2 Phosphorylated on Thr^{160} Possesses Partial Histone H1 Kinase Activity—CDK2 histone H1 kinase activity in the presence and absence of cyclin A3 was assayed before and after phosphorylation by CAK1 (Fig. 3*a*). Both unmodified CDK2 and GST-CAK1 showed no histone H1 kinase activity (Fig. 3*a*, *lanes 3* and *2*, respectively). CDK2 phosphorylated by CAK1 exhibited partial histone H1 kinase activity (Fig. 3*a*, *lane 1*). This activity was comparable with that of the unmodified CDK2-cyclin A3 complex (Fig. 3*a*, *lane 5*). Phosphorylated CDK2 incubated with cyclin A3 showed maximal histone H1 kinase activity (Fig. 3*a*, *lane 4*). PhosphorImager analysis indicated that the phosphorylated CDK2 and the unmodified CDK2-cyclin A binary complex had 0.3 and 0.2%, respectively, of the activity seen in the fully activated phosphorylated CDK2-cyclin A3 binary complex (data not shown). We investigated the possibility that small amounts of insect cyclin may have co-purified with the CDK2 and provided an apparent activity for the highly purified monomeric phosphorylated CDK2. As little as 1% contamination would be significant, since the fully activated phosphorylated CDK2-cyclin A complex is more active by at least 2 orders of magnitude. Experiments were repeated with GST-CAK1 and CDK2 expressed in *E. coli* cells. Fig. 3*b* shows that the bacterially expressed, monomeric CDK2 phosphorylated by CAK1 also exhibits partial, but significant, histone H1 kinase activity.

CDKs can be inhibited by members of the CKI family (28). $p27^{kip1}$ inhibited the histone H1 kinase activity observed with both the fully active phosphorylated binary complex and the partially active unphosphorylated complex (Fig. 3*c*). The partial histone H1 kinase activity of phosphorylated monomeric CDK2 was also inhibited (Fig. 3*d*).

Fluorescence experiments were performed to determine the dissociation constants between various forms of CDK2 and its substrate histone H1. The binding of histone H1 to CDK2-cyclin A induces a 25% quenching of the intrinsic fluorescence of the complex (Fig. 3*e*). This quenching was used to quantify the interaction between CDK2-cyclin A and histone H1. Titrations were performed using a fixed concentration of kinase with increasing concentrations of substrate. K_d values of 1 and 0.7 μM were calculated for CDK2-cyclin A and phosphorylated CDK2-cyclin A, respectively. Monomeric phosphorylated CDK2 was found to bind histone H1 with very low affinity, with a calculated K_d of about 100 μM. Histone H1 binding to monomeric CDK2 was not detected. The results are summarized in Table II.

ATP Binding to CDK2—Binding of ATP to phosphorylated CDK2 was first monitored by following the quenching of intrinsic tryptophan fluorescence. ATP binding to phosphorylated CDK2 results in quenching of the intrinsic fluorescence by 48%. This value is similar to that reported for unphosphorylated CDK2 (44). The titration curves are shown in Fig. 4*a*, where a fixed concentration of CDK2 (0.2 μM) phosphorylated or not on Thr^{160} was titrated with an increasing concentration of ATP or ADP. The curve fitting carried out using the results of the phosphorylated CDK2 experiment calculates an apparent dissociation constant of 120 nM for ATP. This value is 2-fold lower than that determined for unphosphorylated CDK2 (254 nM). In contrast, as shown in Fig. 4*a*, CDK2 phosphorylation decreases by 4.5-fold the CDK2 affinity for ADP. Curve fitting yields apparent K_d values of 1.4 and 6.7 μM for ADP association with CDK2 and phosphorylated CDK2, respectively.

The fluorescence of Mant-ATP was also used to quantify the binding of ATP to phosphorylated CDK2. We have demonstrated that the binding of Mant-ATP to CDK2 overexpressed in *E. coli* cells results in a 10-fold increase in the Mant-group fluorescence (44). This experiment was repeated using as the source of CDK2 the enzyme expressed in recombinant baculovirus-infected insect cells. The binding of Mant-ATP to either unphosphorylated CDK2 or phosphorylated CDK2 results in an increase in the fluorescence of the Mant-group (Fig. 4*b*). These changes reveal that the highly hydrophobic character and the conformation of the CDK2 active site are not significantly modified by Thr^{160} phosphorylation. A fixed concentration of Mant-ATP or Mant-ADP (0.2 μM) was titrated by increasing the CDK2 concentration (Fig. 4*b*). The curve fitting yielded K_d values of 256 and 170 nM for Mant-ATP and 1.5 and 5.4 μM for Mant-ADP against unphosphorylated CDK2 and phosphorylated CDK2, respectively. Mant-ATP bound to CDKs can be fully displaced by an excess of unlabeled nucleotide, resulting in a 5-fold decrease in the fluorescence of the Mant-group. As previously published, the dissociation rate of Mant-ATP from CDK2 using a 200-fold excess of ATP occurs according to a single exponential with a rate constant of 5.4×10^{-3} s^{-1} (44). When this experiment was repeated with phosphorylated CDK2, the dissociation rate constant of Mant-ATP was reduced to a value of 3.1×10^{-3} s^{-1} (Fig. 4*c*). The results are summarized in Table II. These displacement experiments confirm that CDK2 phosphorylation increases the enzyme's affinity for ATP.

Cyclin Binding Is Unaffected by Thr^{160} Phosphorylation of CDK2—Cyclin A binding to CDK2 and phosphorylated CDK2 was quantified by using the fluorescence of Mant-ATP previously bound to the kinase. The binding of cyclin A to CDK2 enhanced the bound Mant-ATP fluorescence 3-fold (Fig. 5). The titration curves followed a monophasic pattern, and their fitting yielded K_d values of 52 nM for CDK2-cyclin A and 48 nM for phosphorylated CDK2-cyclin A with a 1:1 (CDK/cyclin) stoichiometry in both cases (Fig. 5). These results show that phosphorylation on Thr^{160} does not modify the affinity of CDK2 for cyclin A and that phosphorylation is not required, as previously proposed (44), for the formation of a CDK2-cyclin A complex. The enhancement of Mant-ATP fluorescence is similar (3-fold) for cyclin A binding to CDK2 or phosphorylated CDK2, and the magnitude of the enhancement suggests that substantial conformational changes in the nucleotide binding site accompany cyclin binding.

Surface plasmon resonance analysis (BIAcore) was also used to compare the cyclin binding properties of CDK2 and phosphorylated CDK2. Because of the difficulty in immobilizing CDK2

c, B-factor plots for CDK2-ATP and phosphorylated CDK2-ATP. The mean main chain B-factor of each residue along the polypeptide chain is shown for unphosphorylated CDK2 (*thin lines*) and phosphorylated CDK2 (*thick lines*). The outstanding regions of difference include the glycine loop (residues 8–18) and the tip of the activation segment (residues 155–165). *d*, detail of the fold of the CDK2-ATP complex. The interaction of Tyr^{159} and Thr^{160}, at the tip of the activation segment, with residues Glu^{12}–Tyr^{15} in the glycine-rich loop is shown. The *coloring scheme* is the same as for *a*.

or cyclin A3 in an active form using the standard amine coupling chemistry, a GST-CDK2 protein expressed in *E. coli* cells was used. The CDK2 fusion protein was captured by immobilized anti-GST immunoglobulin. Analysis of the sensorgram curves (results not shown) gave a K_d of 0.7 nM for the GST/CDK2-cyclin A3 interaction and a value of 0.5 nM for GST-phosphorylated CDK2-cyclin A3. Although these values are probably significantly affected by the use of dimeric GST fusion proteins (see Ref. 49 and "Discussion") they also indicate no significant difference in apparent affinity of phosphorylated CDK2 or of unmodified CDK2 for cyclin A3.

The Phosphorylated CDK2 Structure Reveals Activation Segment Disorder—Initial crystallization trials with phosphorylated CDK2 were not successful. However, conditions similar to those required to produce CDK2 crystals were able to sustain crystal growth in microseeding experiments with nuclei obtained from nonphosphorylated CDK2 crystals. We have determined structures for phosphorylated CDK2 (results not shown), the ATP-phosphorylated CDK2 complex, and unphosphorylated CDK2 in complex with ATP at 2.1-Å resolution. Our own results and those of others have shown that the structure and mobility of monomeric crystalline CDK2 can depend critically on the nature of the ligand bound to the ATP binding site. In order to compare as closely as possible phosphorylated and unphosphorylated CDK2, we determined the structures of the ATP complexes of both forms of the enzyme, using crystals of comparable size, identical crystal soaking conditions, and identical structure refinement protocols. Statistics relating to the quality of the two data sets and of the two refined models are presented in Table I.

The structure of CDK2, first described by DeBondt *et al.* (35), is that of a minimal protein kinase catalytic core, consisting of an N-terminal domain formed principally from β-sheet and a C-terminal domain formed principally from α-helix. ATP binds in the cleft between the two domains (Fig. 6*a*), forming contacts with both N- and C-terminal lobes. The structure of unphosphorylated monomeric CDK2 differs from that of CDK2 in the active phosphorylated binary form in two major respects: the orientation of the C-helix ("PSTAIRE helix"), and the conformation of the "activation segment" between the conserved sequence motifs DFG (Asp^{145}-Phe^{146}-Gly^{147}) and APE (Ala^{170}-Pro^{171}-Glu^{172}). The incorrect orientation of the C-helix in the inactive form of CDK2 prevents the correct conformation of key catalytic residues, while an inappropriate conformation of the activation segment precludes productive association of a polypeptide substrate at the active site. The refined structures of phosphorylated and nonphosphorylated CDK2 in complex with ATP are remarkably similar (root mean square difference for 290 C-α positions = 0.5 Å). For the part of the structure that is well defined by electron density in both cases (all except residues 36–43 and 153–164), no part of the structure had to be built differently in the phosphorylated as compared with the nonphosphorylated structure. Of the two regions excepted above, the former (residues 36–43) could not be traced in either the phosphorylated or the unphosphorylated CDK2-ATP complex and is known to become well defined only in the binary complex of CDK2 with cyclin A (36). The latter region (residues 153–164) can clearly be traced in the nonphosphorylated structure of CDK2 in complex with ATP but has no continuous electron density in the structure of phosphorylated CDK2 in complex with ATP (Fig. 6*b*). The increased mobility of both the activation segment and the glycine-rich loop in the ATP-phosphorylated CDK2 structure as compared with the structure of ATP-CDK2 is reflected in the main chain B-factor values for each of the models in these regions. With the exception of these two regions, the B factor values agree closely for the two models (Fig. 6*c*). The relevance of this change in mobility to the activity of phosphorylated monomeric CDK2 is discussed later.

DISCUSSION

Phosphorylated CDK2 has been prepared by treatment of purified, nonphosphorylated CDK2 expressed in baculovirus-infected insect cells with CAK1 expressed either in *E. coli* or in *S. cerevisiae*. Purified phosphorylated CDK2 exhibited histone H1 kinase activity representing about 0.3% of the activity measured for the fully active phosphorylated CDK2-cyclin A and comparable with that shown by the unmodified CDK2-cyclin A binary complex. The possibility that activity was the result of association of the CDK2 with endogenous insect cell cyclins was excluded by repeating the experiments using CDK2 and GST-CAK1 expressed in *E. coli* cells. Fisher and Morgan (12) could not detect histone H1 kinase activity associated with monomeric phosphorylated CDK2 prepared by treating CDK2 with reconstituted CAK (CDK7-cyclin H), but the activity reported here is below the sensitivity of the curves shown in that paper.

CDK2 has been isolated from synchronized mammalian cell lines in multiple high and low molecular weight complexes by gel filtration analysis (50). Monomeric CDK2 was identified as a mixture of fast and slow migrating forms as analyzed by SDS-PAGE, suggesting that monomeric phosphorylated CDK2 is present in mammalian cells. These results, together with the results described in this paper suggest that monomeric CDK2 phosphorylated on Thr^{160} may be biologically relevant, and as previously proposed (12), there may be alternative assembly pathways to generate a fully active CDK2-cyclin binary complex. We have found that the cyclin-dependent kinase inhibitor $p27^{kip1}$ does inhibit phosphorylated CDK2 as well as the activity observed with both the fully activated phosphorylated binary complex and the partially active unphosphorylated complex. The concentrations of $p27^{kip1}$ required to inhibit monomeric phosphorylated CDK2 are consistent with the observation that $p27^{kip1}$ has a much lower affinity for monomeric CDKs compared with CDK-cyclin complexes (Ref. 51; and see Ref. 52). The biological significance of the low levels of kinase activity associated with monomeric phosphorylated CDK2 remains to be determined.

The phosphorylated CDK2 structure reveals that Thr^{160} phosphorylation is insufficient to fully activate the kinase and provides an explanation for the very low levels of kinase activity observed. The major CDK2 structural changes required for activation are promoted by cyclin association. Protein kinases show significant variation in their dependence on phosphorylation for activity. Significant structural changes that lead to activation in some protein kinases (*e.g.* the insulin receptor tyrosine kinase (32)) can be promoted solely by phosphorylation, whereas other protein kinases (*e.g.* phosphorylase kinase (53)) require no phosphorylation on the activation segment.

Phosphorylated CDK2 is observed to have both higher affinities for ATP and substrate histone H1 and a lower affinity for ADP than the nonphosphorylated CDK2. In the unphosphorylated monomeric CDK2 structure, Thr^{160} is located close to the side chain of Glu^{12}, and the aromatic ring of Tyr^{159} stacks against the planar peptide backbone around Gly^{16} (Fig. 6*d*). The glycine loop structure that favors this set of interactions is also promoted by additional interactions between backbone atoms of residues Glu^{12}–Thr^{14} with the ribose-triphosphate group of ATP. Phosphorylation of Thr^{160} by both steric and charge constraints precludes this set of stabilizing interactions between residues in the glycine-rich loop and the activation segment. In the phosphorylated CDK2 structure, increased structural flexibility extends to residues His^{161}, Glu^{162}, Val^{163}, and Val^{164} in the activation loop. Two structures of protein

kinases in complex with peptide substrates, insulin receptor kinase (32) and phosphorylase kinase (54), show a defined conformation of the protein substrate across the catalytic site. In particular, there is an antiparallel β-sheet between the amino acids in the P+1 and P+3 positions of the protein substrate and those of the activation segment immediately following the negatively charged residue that is responsible for activation (Tyr^{1163} in insulin receptor kinase and Glu^{182} in phosphorylase kinase). The structural results show that the increased mobility of the activation segment in phosphorylated CDK2 compared with the unmodified CDK2 structure results in accessibility of the catalytic site for binding substrate and a potential for the kinase to adopt the active conformation, albeit for a short time and for a small proportion of the population, when in solution. This structural mobility may contribute to the observed higher affinity of phosphorylated CDK2 for ATP and histone H1 and its observed lower affinity for ADP than unmodified CDK2. Fluorescence studies support this structural interpretation and suggest mechanisms by which phosphorylation of Thr^{160} could enhance CDK2's catalytic activity. It is assumed that, upon crystallization, the more thermodynamically stable and more prevalent inactive conformation of phosphorylated CDK2 has been selected.

In contrast, phosphorylation of CDK2 does not significantly alter its affinity for cyclin A. Using fluorescence methods, CDK2 and phosphorylated CDK2 showed high affinity for cyclin A with measured K_d values of 52 and 48 nM for phosphorylated CDK2-cyclin A and CDK2-cyclin A association, respectively. Repeating the measurements using BIAcore analysis gave K_d values of 0.7 nM for phosphorylated CDK2-cyclin A and 0.5 nM for CDK2-cyclin A. These results confirmed that the two CDK2 species have comparable affinity for cyclin A. The low values observed for K_d in the BIAcore experiments may be an artifact produced by the use of GST-CDK2. Ladbury *et al*. (49) have shown that avidity effects that result from the dimerization of GST fusion proteins could be responsible for overestimates of affinities measured by surface plasmon resonance.

We have shown that CAK1 phosphorylates monomeric CDK2 more effectively than the binary CDK2-cyclin A complex. This observation is consistent with structural results. Although the structure of CAK1 is not yet known, it is anticipated to have the kinase fold reported for the 14 protein kinase structures determined to date by x-ray crystallographic analysis. Different protein kinases may demand slightly different substrate conformations, as seems to be the case for the cAPK-peptide inhibitor complex (55) and for CDKs that recognize Ser/Thr-Pro motifs. However, the structural conservation of the catalytic sites in the active kinase conformations suggests, as discussed above, that the protein substrate needs to be able to adopt an approximately extended conformation for recognition.

In the CDK2-cyclin A complex, residues 159–162 around Thr^{160} adopt a turn of 3_{10} helix (36). A conformational change would be required for this region to adapt to the activating kinase catalytic site if an extended conformation is required for recognition, although Thr^{160} itself is accessible. In unmodified CDK2, although the preferred conformation of the activation segment buries Thr^{160}, the region exhibits considerable mobility (Fig. 6*c*). This mobility would allow displacement of Thr^{160} from its buried position and provide scope for the activation segment to adapt its conformation to the CAK1 catalytic site. Just such an adaptation occurs when the mobile N-terminal region of glycogen phosphorylase *b* adapts to the catalytic site of phosphorylase kinase (54). $p27^{kip1}$ binding to the binary complex promotes phosphorylation of Thr^{160} by CAK1. This result is in contrast to the ability of $p27^{kip1}$ when bound to CDK2-cyclin E complexes to inhibit phosphorylation of Thr^{160} by CAK (56). Although there is no structural information about the unphosphorylated ternary complex of CDK2-cyclin A-$p27^{kip1}$ our results suggest that the mobility of the activation loop is enhanced in this complex. In the phosphorylated CDK2-cyclin A-$p27^{kip1}$ complex (57), the $p27^{kip1}$ inhibitor contacts both cyclin A and CDK2, causing significant conformational changes in CDK2 that result in displacement of the β1 and β2 strands and the glycine loop.

The notion of increased mobility in the activation segment in phosphorylated CDK2 compared with phosphorylated CDK2-cyclin A may also explain the catalytic activity of KAP. It has been shown that KAP will not dephosphorylate the binary phosphorylated CDK2-cyclin A complex but only monomeric phosphorylated CDK2 (24). In the phosphorylated CDK2-cyclin A structure, the phospho-Thr^{160} is buried, and the activation segment is well localized so that it would be difficult for the phosphatase to have access to the phosphothreonine. In monomeric phosphorylated CDK2, the activation segment is mobile and available for modification by KAP.

In summary, the mobility of the activation segment in phosphorylated CDK2 observed in the crystal structure analysis provides an explanation for the effects observed *in vitro* with purified enzymes. We have shown that phosphorylated CDK2 has basal activity, that monomeric CDK2 is a better substrate than CDK2-cyclin A for CAK1, and that phosphorylated CDK2 and unmodified CDK2 have similar affinities for cyclin A. The significance of these results for the *in vivo* situation remains to be evaluated.

Acknowledgments—We acknowledge with gratitude the help of the beamline scientists at X-ray Diffraction Elettra (Trieste); BW7B, DESY (Hamburg); and 9.5, SRS (Daresbury). We thank Carol Robinson and Paula Tito for the mass spectroscopic analysis of phosphorylated CDK2. We thank David Morgan for the gift of the baculoviral construct expressing human CDK2, Carl Mann for various constructs expressing CAK1, Neil Hanlon for KAP, and Tim Hunt for the cyclin A3 and GST-CDK2 constructs together with much stimulating discussion. At the Laboratory of Molecular Biophysics (Oxford), we thank Stephen Lee, Richard Bryan, Kathryn Measures, and Irene Taylor for assistance.

REFERENCES

1. Morgan, D. O. (1997) *Annu. Rev. Cell Dev. Biol.* **13,** 261–291
2. Desai, D., Gu, Y., and Morgan, D. O. (1992) *Mol. Biol. Cell* **3,** 571–582
3. Connell-Crowley, L., Solomon, M. J., Wei, N., and Harper, W. J. (1993) *Mol. Biol. Cell* **4,** 79–92
4. Gould, K. L., Moreno, S., Owen, D. J., Sazer, S., and Nurse, P. (1991) *EMBO J.* **10,** 3297–3309
5. Krek, W., and Nigg, E. A. (1992) *New Biol.* **4,** 323–329
6. Gu, Y., Rosenblatt, J., and Morgan, D. O. (1992) *EMBO J.* **11,** 3995–4005
7. Solomon, M. (1993) *Curr. Opin. Cell Biol.* **5,** 180–186
8. Ducommmun, B., Brambilla, P., Felix, M.-A., Franza, B. R., Jr., Karsenti, E., and Draetta, G. (1991) *EMBO J.* **10,** 3311–3319
9. Fesquet, D., Labbe, J.-C., Derancourt, J., Capony, J.-P., Galas, S., Girard, F., Lorca, T., Shuttleworth, J., Doree, M., and Cavadore, J.-C. (1993) *EMBO J.* **12,** 3111–3121
10. Solomon, M. J., Harper, J. W., and Shuttleworth, J. (1993) *EMBO J.* **12,** 3133–3142
11. Poon, R. Y. C., Yamashita, K., Adamczewski, J. P., Hunt, T., and Shuttleworth, J. (1993) *EMBO J.* **12,** 3123–3132
12. Fisher, R. P., and Morgan, D. O. (1994) *Cell* **78,** 713–724
13. Makela, T. P., Tassan, J.-P., Nigg, E. A., Frutiger, S., Hughes, G. J., and Weinberg, R. A. (1994) *Nature* **371,** 254–257
14. Tassan, J.-P., Jaquenoud, M., Fry, A. M., Frutiger, S., Hughes, G. J., and Nigg, E. A. (1995) *EMBO J.* **14,** 5608–5617
15. Fisher, R. P., Jin, P., Chamberlin, H. M., and Morgan, D. O. (1995) *Cell* **83,** 47–57
16. Devault, A., Martinez, A.-M., Fesquet, D., Labbe, J.-C., Morin, N., Tassan, J.-P., Nigg, E. A., Cavadore, J.-C., and Doree, M. (1995) *EMBO J.* **14,** 5027–5036
17. Shiekhattar, R., Mermelstein, F., Fischer, R. P., Drapkin, R., Dynlacht, B., Wessling, H. C., Morgan, D. O., and Reinberg, D. (1995) *Nature* **374,** 283–287
18. Serizawa, H., Makela, T. P., Conaway, J. W., Conaway, R. C., Weinberg, R. A., and Young, R. A. (1995) *Nature* **374,** 280–282
19. Kaldis, P., Sutton, A., and Solomon, M. J. (1996) *Cell* **86,** 553–564
20. Thuret, J.-Y., Valay, J.-G., Faye, G., and Mann, M. (1996) *Cell* **86,** 565–576
21. Espinoza, F. H., Farrell, A., Erdjument-Bromage, H., Tempst, P., and Morgan, D. O. (1996) *Science* **273,** 1714–1717
22. Gyuris, J., Golemis, E., Chertkov, H., and Brent, R. (1993) *Cell* **75,** 791–803

23. Hannon, G. J., Casso, D., and Beach, D. (1994) *Proc. Natl. Acad. Sci. U. S. A.* **91,** 1731–1735
24. Poon, R. Y. C., and Hunter, T. (1995) *Science* **270,** 90–93
25. Murray, A. (1995) *Cell* **81,** 149–152
26. Hershko, A. (1997) *Curr. Opin. Cell Biol.* **9,** 788–799
27. Krek, W. (1998) *Curr. Opin. Genet. Dev.* **8,** 36–42
28. Sherr, C. J., and Roberts, J. M. (1995) *Genes Dev.* **9,** 1149–1163
29. Knighton, D. R., Zheng, J., Ten Eyck, L. F., Ashford, V. A., Xuong, N.-H., Taylor, S. S., and Sowadski, J. M. (1991) *Science* **253,** 407–413
30. Bossmeyer, D., Engh, R. A., Kinzel, V., Ponstingl, H., and Huber, R. (1993) *EMBO J.* **12,** 849–859
31. Yamaguchi, H., and Hendrickson, W. A. (1996) *Nature* **384,** 484–489
32. Hubbard, S. R. (1997) *EMBO J.* **16,** 5572–5581
33. Canagarajah, B. J., Khokhlatchev, A., Cobb, M. H., and Goldsmith, E. J. (1997) *Cell* **90,** 859–869
34. Martinez, A.-M., Afshar, M., Martin, F., Cavadore, J.-C., Labbe, J.-C., and Doree, M. (1997) *EMBO J.* **16,** 343–354
35. De Bondt, H. L., Rosenblatt, J., Jancarik, J., Jones, H. D., Morgan, D. O., and Kim, S.-H. (1993) *Nature* **363,** 595–602
36. Jeffrey, P. D., Russo, A. A., Polyak, K., Gibbs, E., Hurwitz, J., Massague, J., and Pavletich, N. P. (1995) *Nature* **376,** 313–320
37. Russo, A., Jeffrey, P. D., and Pavletich, N. P. (1996) *Nat. Struct. Biol.* **3,** 696–700
38. Brown, N. R., Noble, M. E. M., Endicott, J. A., Garman, E. F., Wakatsuki, S., Mitchell, E. P., Rasmussen, B., Hunt, T., and Johnson, L. N. (1995) *Structure* **3,** 1235–1247
39. Rosenblatt, J., De Bondt, H., Jancarik, J., Morgan, D. O., and Kim, S.-H. (1993) *J. Mol. Biol.* **230,** 1317–1319
40. Hiratsuka, T. (1983) *Biochim. Biophys. Acta* **742,** 496–508
41. John, J., Sohmen, R., Feuerstein, J., Linke, R., Wittinghofer, A., and Goody, R. S. (1990) *Biochemistry* **29,** 6058–6065
42. Lorca, T., Labbe, J.-C., Devault, A., Fesquet, D., Strausfeld, U., Nilsson, J., Nygren, P.-A., Uhlen, M., Cavadore, J.-C., and Doree, M. (1992) *J. Cell Sci.* **102,** 55–62
43. Divita, G., Goody, R. S., Gautheron, D. C., and Di Pietro, A. (1993) *J. Biol. Chem.* **268,** 13178–13186
44. Heitz, A., Morris, M. C., Fesquet, D., Cavadore, J.-C., Doree, M., and Divita, G. (1997) *Biochemistry* **36,** 4995–5003
45. Otwinowski, Z. (1993) in *Data Collection and Processing* (Sawyer, L., Isaacs, N., and Bailey, S., eds) pp. 56–62, SERC Laboratory, Daresbury, Warrington, UK
46. Jones, T. A., Zou, J. Y., Cowan, S. W., and Kjeldgaard, M. (1991) *Acta Crystallogr. Sec. A* **47,** 110–119
47. Murshudov, G. N., Vagen, A. A., and Dodson, E. J. (1997) *Acta Crystallogr. Sec. D* **53,** 240–255
48. Lamzin, V. S., and Wilson, K. S. (1993) *Acta Crystallogr. Sec. D* **49,** 129–147
49. Ladbury, J. E., Lemmon, M. A., Zhou, M., Green, J., Botfield, M. C., and Schlessinger, J. (1995) *Proc. Natl. Acad. Sci. U. S. A.* **92,** 3199–3203
50. Rosenblatt, J., Gu, Y., and Morgan, D. O. (1992) *Proc. Natl. Acad. Sci. U. S. A.* **89,** 2824–2828
51. Polyak, K., Kato, J., Solomon, M. J., Sherr, C. J., Massague, J., Roberts, J. M., and Koff, A. (1994) *Genes Dev.* **8,** 9–22
52. Harper, J. W., Elledge, S. J., Keyomarsi, K., Dynlacht, B., Tsai, L.-H., Zhang, P., Dobrowolski, S., Bai, C., Connell-Crowley, L., Swindell, E., Fox, M. P., and Wei, N. (1995) *Mol. Biol. Cell* **6,** 387–400
53. Owen, D. J., Noble, M. E. M., Garman, E. F., Papageorgiou, A. C., and Johnson, L. N. (1995) *Structure* **3,** 467–482
54. Lowe, E. D., Noble, M. E. M., Skamnaki, V. T., Oikonomakos, N. G., Owen, D. J., and Johnson, L. N. (1997) *EMBO J.* **16,** 6646–6658
55. Knighton, D. R., Zheng, J., Ten Eyck, L. F., Xuong, N.-H., Taylor, S. S., and Sowadski, J. M. (1991) *Science* **253,** 414–420
56. Polyak, K., Lee, M.-H., Erdjument-Bromage, H., Koff, A., Roberts, J. M., Tempst, P., and Massague, J. (1994) *Cell* **78,** 59–66
57. Russo, A. A., Jeffrey, P. D., Patten, A. K., Massague, J., and Pavletich, N. P. (1996) *Nature* **382,** 325–331